Available online at www.sciencedirect.com

SCIENCE DIRECT®

Journal of Nuclear Materials 352 (2006) 151–156

journal of nuclear materials

www.elsevier.com/locate/jnucmat

Fabrication method and thermal conductivity assessment of molybdenum-precipitated uranium dioxide pellets

Si-Hyung Kim [a,*], Chang-Young Joung [a], Han-Soo Kim [a], Young-Woo Lee [a], Ho-Jin Ryu [a], Dong-Seong Sohn [a], Dong-Joo Kim [b]

[a] *Korea Atomic Energy Research Institute, P.O. Box 105, Yuseong, Daejeon 305-600, South Korea*
[b] *Department of Nuclear Engineering, Hanyang University, Seoul 133-791, South Korea*

Abstract

UO_2 pellets containing molybdenum networks were fabricated when UO_2 pellets mixed with 3 or 5 wt% MoO_3 powder were sintered in the CO_2/CO ratio of 19/1 and then annealed in an H_2 atmosphere. The thermal diffusivities of UO_2 and Mo-precipitated UO_2 pellets were measured in the range of 298–1673 K by a laser flash method and their thermal conductivities were calculated from the thermal diffusivity, the sample density and the published specific heat capacity data. The temperature dependency of the thermal conductivity up to 1673 K in UO_2 and Mo-precipitated UO_2 was found to be modeled well using the conductivity equation, $\kappa = (A + BT)^{-1}$. The thermal conductivity of the Mo-precipitated UO_2 was higher than that of the pure UO_2.

PACS: 66.70; 81.05.M

---

1. Introduction

Thermal conductivity is one of the most important properties of UO_2 fuel pellets as it influences the fuel operating temperatures, in turn affecting directly fuel performance and behavior, particularly with respect to fission gas release and swelling. The thermal conductivity of UO_2 is very low when compared with U metal, UN [1] or UC [2], however, various efforts have been attempted to enhance the thermal conductivity of the UO_2 pellets [3].

It is well known that the thermal conductivity of ceramic oxides can be increased by fabricating the Cermet (ceramic-metal) [4]. Mo compounds can be present as Mo metal or Mo oxides according to the oxygen partial pressures at high temperatures and have a low neutron absorption cross-section. The melting point of Mo metal is higher than that of Mo oxides and therefore Mo-containing cermet fuels can be used even up to very high temperature.

This work deals with the fabrication method and the thermal conductivity measurement of Mo-precipitated UO_2 pellets in which molybdenum network is continuously formed over the entire or some parts of a sintered body. The thermal conductivities of UO_2 and Mo-precipitated UO_2 pellets

---

[*] Corresponding author. Tel.: +82 42 868 2514; fax: +82 42 868 8868.
E-mail address: exodus@kaeri.re.kr (S.-H. Kim).

0022-3115/$ - see front matter © 2006 Elsevier B.V. All rights reserved.
doi:10.1016/j.jnucmat.2006.02.049

were determined from room temperature to 1673 K.

2. Experimental

The starting materials were IDR-UO_2 (Integrated Dry Route) powder purchased from BNFL (British Nuclear Fuels plc) and MoO_3 powder with a purity of 99.9 % (Aldrich Chemical Company). The UO_2 powder [5,6] was mixed with measured amounts of MoO_3 powder, in concentrations varying from 0.1 to 5 wt% MoO_3, by a Turbula® mixer for 1 h and then successively milled by a planetary mill for 1/2 h. The milled oxide powders were compacted with a compaction pressure of 300 MPa and the green pellet specimens were sintered between 1773 and 1973 K in H_2 with a dew point of 243 K or CO_2/CO ratios of 19/1 and 1/1. All the pellets sintered in the CO_2/CO atmosphere were reduced at each sintering temperature in an H_2 atmosphere to convert Mo oxides to Mo metal.

The thermal diffusivity was measured by a laser flash method (Netzsch LFA-417). The thermal diffusivity of UO_2 and UO_2–3wt%MoO_3 was measured from 298 to 1673 K, and that of UO_2–5wt%MoO_3 was measured only up to 1573 K. The measurements of the thermal diffusivity were carried out three times at every test temperature step in a vacuum at a pressure of less than 10^{-5} Pa. The average value of these three measurements was used and the experimental uncertainty associated with these measurements was within 5%. For the thermal diffusivity measurements, samples were prepared in the shape of discs with an 8 mm diameter and 1 mm thickness. A pulse of a laser was projected on to the front surface of the pellet and the temperature rise on the rear side of the pellet was recorded as a transient signal by using an infrared detector. The thermal diffusivity (D) was calculated from the following relationship:

$$D = \frac{W}{\pi}\frac{L^2}{t_{1/2}}, \tag{1}$$

where $t_{1/2}$ is the time in seconds to one-half of the maximum temperature rise at the rear surface of the sample and L is the sample thickness in mm. W is a dimensionless parameter which is a function of the relative heat loss from the sample during the measurement and the value of W is 0.1388 in the absence of heat loss. The thermal conductivities were calculated from the heat capacity, the sample density and the thermal diffusivity.

3. Results and discussion

3.1. Fabrication of Mo-precipitated UO_2

Fig. 1 shows the oxygen potential of the stoichiometric UO_2, Mo/MoO_2, Mo/MoO_3 and three sintering atmospheres corresponding to H_2 with a dew point of 243 K and CO_2/CO ratios of 1/1 and 19/1 [7,8]. According to Fig. 1, Mo metal, MoO_2 and MoO_3 are stable in H_2 and CO_2/CO ratios of 1/1 and 19/1, respectively. The melting points of Mo metal, MoO_2 and MoO_3 are 2896, 2200 and 1073 K, respectively, and therefore it can be predicted that a mixture of UO_2 and MoO_3 powders will show a liquid phase sintering behavior above the melting point of MoO_3 powder in the CO_2/CO ratio of 19/1.

Fig. 2 shows the microstructures of UO_2 and UO_2–0.1wt%MoO_3 pellets sintered in H_2 and CO_2/CO ratios of 1/1 and 19/1. When the UO_2–0.1wt%MoO_3 compact was sintered at 1973 K in an H_2 atmosphere, the MoO_3 powders would be reduced to Mo metal during the initial sintering. In this case, the Mo metals cannot increase the grain size of UO_2 pellet during the sintering because those may be obstacle to the grain boundary movement. However, the grain sizes of UO_2 and UO_2–0.1wt%MoO_3 sintered in H_2 were about the same at 8 μm. Mo metals cannot be seen in UO_2–0.1wt%MoO_3 pellet because the Mo metals were evaporated during the thermal etching in a CO_2 atmosphere. UO_2–MoO_3 compact would be converted to UO_2–MoO_2 when that was sintered at

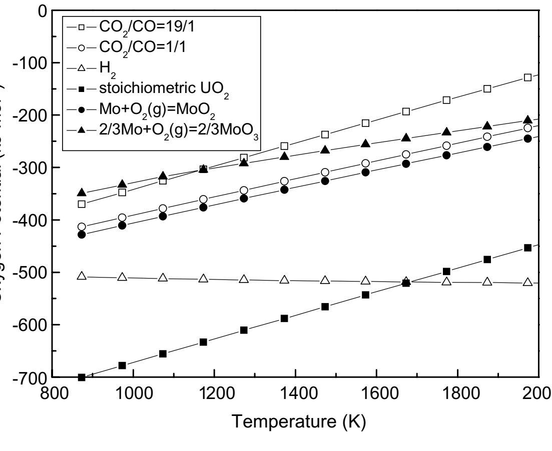

Fig. 1. Oxygen potential of stoichiometric UO_2, Mo/MoO_2, Mo/MoO_3 and three sintering atmospheres corresponding to H_2 and CO_2/CO ratios of 1/1 and 19/1.

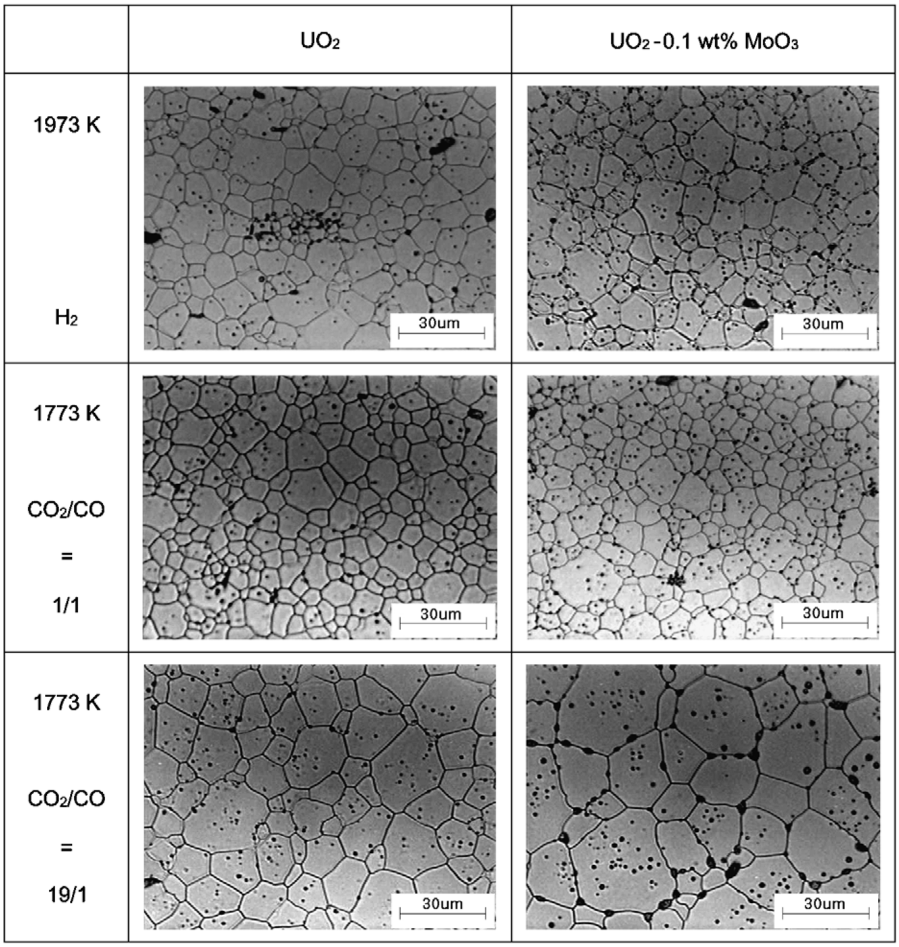

Fig. 2. The microstructures of UO_2 and UO_2 mixed with 0.1 wt% MoO_3 sintered in H_2 and CO_2/CO ratios of 1/1 and 19/1.

1573 K in the CO_2/CO ratio of 1/1. These MoO_2 did not also enhance the grain growth of UO_2.

By the way, MoO_3 powder will be present as a liquid phase at 1573 K in the CO_2/CO of 19/1 and so the grain growth in UO_2–0.1wt%MoO_3 can be accelerated by the liquid phase sintering. Nonetheless, molybdenum networks were not observed in this UO_2–0.1wt%MoO_3 because of the low volume fraction of MoO_3. In the end, UO_2 and UO_2–0.1wt%MoO_3 sintered in the CO_2/CO ratio of 19/1 have the grain sizes of 11 and 18 μm, respectively.

The MoO_3 fraction was increased more than 1 wt% in order to make UO_2 pellets containing molybdenum network. Fig. 3 shows the microstructures, before the thermal etching, of UO_2 and UO_2 mixed with 3 or 5 wt% MoO_3 sintered at 1873 K in the CO_2/CO ratio of 19/1. It can be readily seen that Mo networks are formed along the grain boundary in these UO_2–MoO_3 pellets. As mentioned before, MoO_3 has not only a low melting point but also a low boiling point and so there is a difference in the microstructures between the inner and surface region of the UO_2–MoO_3 pellets. For example, in the surface region, not only was the grain size so small (about 8 μm), but also Mo metals could not be seen. On the contrary, in the inner region, Mo networks were formed along the grain boundary and the grain size was 30–40 μm. This phenomenon is considered to happen by the evaporation of the MoO_3 phase. UO_2 will have open structure in the pellet surface during the initial sintering stage and in this case, the MoO_3 phase distributed in the pellet surface region may be easily evaporated and therefore may not affect the grain growth of the UO_2. On the other hand, the MoO_3 phase located in the inner region of the pellet will

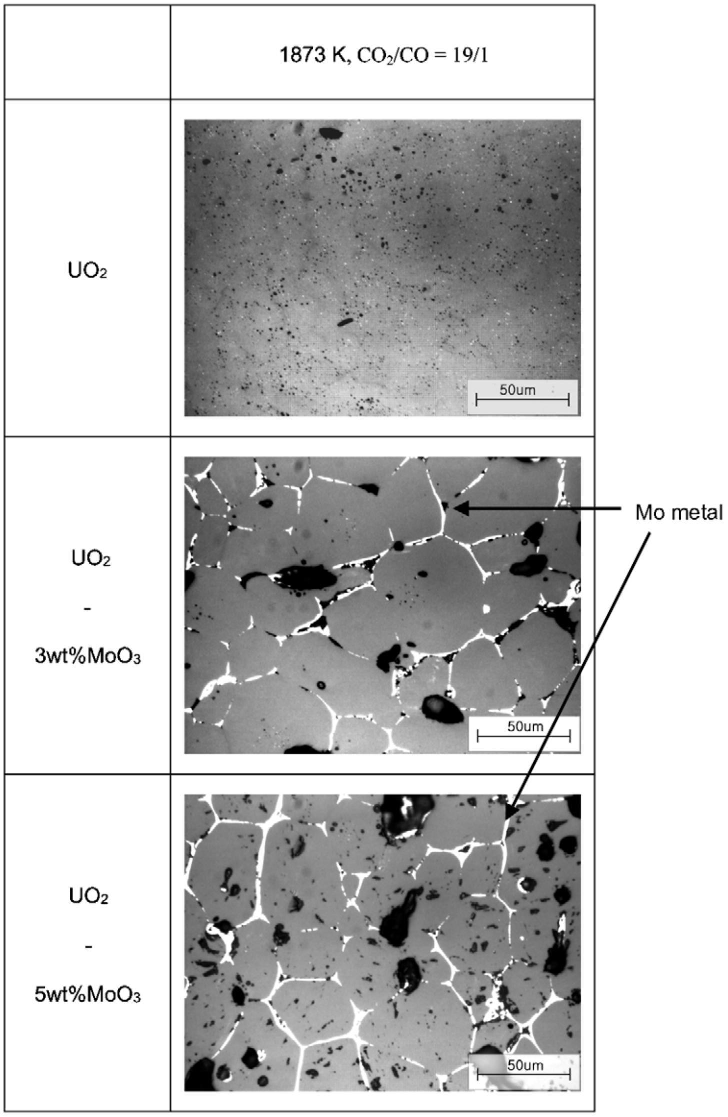

Fig. 3. The microstructures of UO_2 and UO_2 mixed with 3 or 5 wt% MoO_3 sintered in the CO_2/CO ratio of 19/1.

not be easily evaporated and can enhance the grain growth of UO_2. The MoO_3 fraction is related to the volume fraction of the liquid and this has a significant influence on the sintering rate and the microstructure of UO_2. That is to say, densification and grain growth depend on the amount of the liquid phase because the liquid connectivity depends on the volume fraction of the liquid and the diffusion of a solid phase is through this liquid phase [9]. Therefore, Fig. 3 shows the inner region of UO_2–MoO_3 sintered pellets. The sintered density of the UO_2, UO_2–3wt%MoO_3 and UO_2–5wt%MoO_3 pellets were 96.2, 87.3 and 82.0% TD, respectively.

Mo metal powder instead of MoO_3 as a starting material can also be used to fabricate the Mo-containing Cermet pellets. In this case, sintering conditions such as CO_2/CO ratio and sintering temperature should be a little modified.

3.2. Thermal conductivity

Fig. 4 shows the thermal diffusivities of UO_2 and Mo-precipitated UO_2 pellets as a function of the temperature. The data of all the samples were normalized to 95% of the theoretical density by using the following equation [10]:

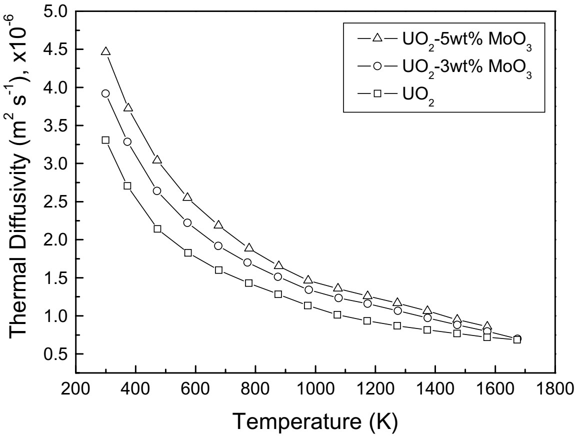

Fig. 4. The thermal diffusivities of UO_2 and Mo-precipitated UO_2 pellets as a function of the temperature.

$$D_{95} = \frac{D_{\mathrm{M}}[(1-0.05\eta)(1-P)]}{[(1-\eta P)(1-0.05)]}, \tag{2}$$

where D_{M}, η and P are, respectively, the measured thermal diffusivity, the experimentally determined fit parameter including its temperature dependency, and the porosity of the sample. Here, for the value of η, which is a function of T, the following equation suggested by Brandt and Neuer [11] was used:

$$\eta = 2.6 - 5\times 10^{-4}\ (T - 273.15), \tag{3}$$

where T is the absolute temperature. The thermal diffusivities of UO_2 and Mo-precipitated UO_2 pellets gradually decreased with the test temperature, as shown in Fig. 4. Fig. 4 also shows the dependency of the thermal diffusivity as a function of the MoO_3 content. The thermal diffusivity of the Mo-precipitated UO_2 pellets increased with an increase of the MoO_3 content.

The thermal conductivity (κ) was calculated from the measured thermal diffusivity (D), specific heat capacity (C_{P}) and sample density (ρ) using the following relationship:

$$\kappa = DC_{\mathrm{P}}\rho. \tag{4}$$

The heat capacities of Mo-precipitated UO_2 pellets have not been available in any literature, so they were estimated from those of individual component materials using the following expression (Neumann–Kopp equation):

$$C = \sum_i X_i C_i, \tag{5}$$

where X_i and C_i are the volume fraction and the heat capacity of the component i, respectively. The specific heat capacity of pure UO_2 is available from the International Nuclear Safety Center (INSC) database of the Argonne National Laboratory on the World-Wide Web [12] and that of Mo is taken from the software [8] which is a tool with extensive thermo-chemical database. The thermal expansion data of Mo-precipitated UO_2, which are required to calculate the temperature dependence of the bulk densities, are also not available. In composite materials like Mo-precipitated UO_2, the metal component does not influence the thermal expansion of the ceramic lattice because the two components do not form the solid solution. In the present study, therefore, the linear thermal expansion data of UO_2 recommended by the literature [12] was used to calculate the temperature dependence of bulk densities of UO_2–MoO_3 pellets.

The thermal conductivity normalized to 95% TD as a function of the temperature is shown in Fig. 5. The data for UO_2 agree well with the reported values [12] for the entire temperature range of this study. The thermal conductivities of all the pellets decrease gradually with the increase of the temperature as shown in Fig. 5. As the temperature increases, the phonon–phonon scattering increases and thus the phonon mean free path decreases, resulting in a decrease in the thermal conductivity. Like the results of the thermal diffusivity, the thermal conductivities of Mo-precipitated UO_2 also increased with an increase of the MoO_3.

In general, a phonon–phonon scattering and a phonon-impurity scattering are the dominant mechanisms for a thermal conductivity in a non-conductive solid (ceramics). Klemens [13] has proposed a

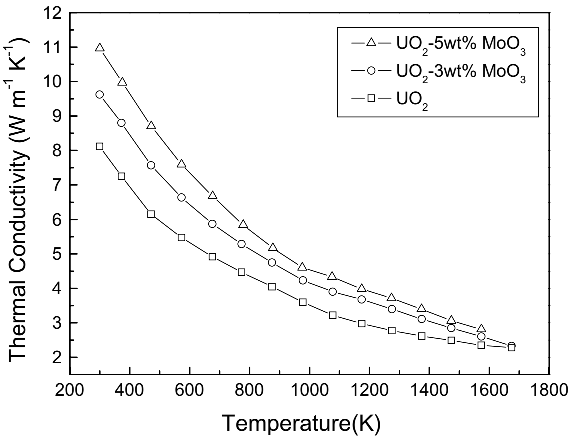

Fig. 5. The thermal conductivity normalized to 95% TD using Eq. (6) as a function of the temperature.

Table 1
Measured values of A and B in Eq. (6) for the UO_2 and UO_2–Mo pellets

MoO_3 content (wt%)	A (m K W^{-1})	B (m W^{-1})
0	0.05253	0.00023
3	0.0417	0.0002
5	0.03378	0.00018

heat conduction model in materials where a phonon–phonon (Umklapp) scattering and a phonon-impurity scattering occur simultaneously. If the additive resistance approximation is assumed, the thermal conductivity of insulating solids is given by the following equation [13,14].

$$\kappa = (A + BT)^{-1}, \tag{6}$$

where T is the absolute temperature and A and B are constants that are related to the phonon-impurity and phonon–phonon (Umklapp) scattering processes, respectively. Eq. (6) reflects the fact that, above the Debye temperature, a phonon–phonon scattering is proportional to the temperature, whereas a phonon-impurity scattering can normally be assumed to be independent of the temperature. Values of A and B can be determined by a least squares fit of Eq. (6) to the thermal conductivity data. Eq. (6) does not express very well the quantitative relation between the thermal conductivity and the content of the impurities in the sample, but Eq. (6) models the observed temperature dependency well.

Table 1 shows the values of A and B of UO_2 and Mo-precipitated UO_2 pellets determined by fitting the thermal conductivity data to Eq. (6). The values of A and B decreased gradually with an increase of the MoO_3 content.

4. Summary

UO_2 pellets containing molybdenum metal networks were fabricated from the UO_2–MoO_3 powder mixtures and the thermal diffusivities of UO_2 and Mo-precipitated UO_2 pellets were measured from room temperature to 1673 K by a laser flash method.

1. MoO_3 powder was reduced to Mo metal and MoO_2 phase at high temperatures in H_2 and CO_2/CO ratio of 1/1, respectively. These Mo metals and MoO_2 phases did not increase the grain size of the UO_2 pellet during the sintering.
2. When UO_2 pellets mixed with 3 or 5 wt% MoO_3 were sintered in the CO_2/CO ratio of 19/1, large grain growth took place and Mo networks were formed along the grain boundary, principally in the inner region of these pellets.
3. Thermal conductivity of the Mo-precipitated UO_2 pellets was higher than that of the pure UO_2 pellet and increased with an increase of the MoO_3 fraction.

Acknowledgements

The authors acknowledge that this work has been carried out under the Nuclear R&D Program supported by the Ministry of Science and Technology in South Korea.

References

[1] S.B. Ross, M.S. El-Genk, B. Matthews, J. Nucl. Mater. 151 (1988) 318.
[2] R.D. Coninck, W.V. Lierde, A. Gijs, J. Nucl. Mater. 57 (1975) 69.
[3] J.H. Yang, K.W. Song, K.S. Kim, Y.H. Jung, in: Proc. Korean Nucl. Soc. Autumn Meeting, October 2004.
[4] P. Weimar, F. Thummler, H. Bumm, J. Nucl. Mater. 31 (1969) 215.
[5] H.S. Kim, S.H. Kim, Y.W. Lee, S.H. Na, J. Korean Nucl. Soc. 28 (1996) 458.
[6] S.H. Na, S.H. Kim, Y.W. Lee, M.J. Yoo, J. Korean Nucl. Soc. 34 (2002) 433.
[7] T.B. Lindemer, T.M. Besmann, J. Nucl. Mater. 130 (1985) 473.
[8] Outokumpu HSC Chemistry for Windows Ver. 4.1 (software), 1999.
[9] R.M. German, Liquid Phase Sintering, Plenum, New York and London, 1985, p. 181.
[10] M. Hirai, S. Ishimoto, J. Nucl. Sci. Technol. 28 (1991) 995.
[11] R. Brandt, G. Neuer, J. Non-Equilib. Thermodyn. 1 (1976) 3.
[12] World Wide Web, INSC Materials Properties Database. Available from: <http://www.insc.anl.gov/matprop/>.
[13] P.G. Klemens, Proc. Phys. Soc. A68 (1955) 1113.
[14] W.D. Kingery, J. Am. Ceram. Soc. 42 (1959) 617.